Regenerative Therapy 21 (2022) 477–485

Contents lists available at ScienceDirect

Regenerative Therapy

journal homepage: http://www.elsevier.com/locate/reth

Original Article

miR-30a inhibits the osteogenic differentiation of the tibia-derived MSCs in congenital pseudarthrosis via targeting HOXD8

Weihua Ye, Yiyong Huang, Guanghui Zhu, An Yan, Yaoxi Liu, Han Xiao, Haibo Mei*

Department of Orthopaedics, Hunan Children's Hospital, Changsha 410007, Hunan Province, PR China

ARTICLE INFO

Article history:
Received 21 July 2022
Received in revised form
2 September 2022
Accepted 12 September 2022

Keywords:
Congenital pseudarthrosis of the tibia
miR-30a
HOXD8
RUNX2

ABSTRACT

Background: Congenital pseudarthrosis of the tibia (CPT) is an uncommon congenital deformity and a special subtype of bone nonunion. The lower ability of osteogenic differentiation in CPT-derived mesenchymal stem cells (MSCs) could result in progression of CPT, and miR-30a could inhibit osteogenic differentiation. However, the role of miR-30a in CPT-derived MSCs remains unclear.

Methods: The osteogenic differentiation of CPT-derived MSCs treated with the miR-30a inhibitor was tested by Alizarin Red S staining and alkaline phosphatase (ALP) activity. The expression levels of protein and mRNA were assessed by Western blot or quantitative reverse transcription-polymerase chain reaction (RT-qPCR), respectively. The interplay between miR-30a and HOXD8 was investigated by a dual-luciferase reporter assay. Chromatin immunoprecipitation (ChIP) was conducted to assess the binding relationship between HOXD8 and RUNX2 promoter.

Results: CPT-derived MSCs showed a lower ability of osteogenic differentiation than normal MSCs. miR-30a increased in CPT-derived MSCs, and miR-30a downregulation promoted the osteogenic differentiation of CPT-derived MSCs. Meanwhile, HOXD8 is a direct target for miR-30a, and HOXD8 could transcriptionally activate RUNX2. In addition, miR-30a could inhibit the osteogenic differentiation of CPT-derived MSCs by negatively regulating HOXD8.

Conclusion: miR-30a inhibits the osteogenic differentiation of CPT-derived MSCs by targeting HOXD8. Thus, this study might supply a novel strategy against CPT.

1. Introduction

Congenital pseudarthrosis of the tibia (CPT) is one of the most challenging problems in pediatric orthopedics [1,2]. The incidence rate of CPT is between 1:140,000 and 1:250,000 births. Clinically, CPT mostly manifests as progressive varus and antecurvation malformation of the tibia in infancy and childhood. CPT is associated with neurofibromatosis or fibrous dysplasia [3,4]. Accumulating evidence has revealed that a pathological alteration of the periosteum in pseudarthrosis may be crucially responsible for CPT [4,5]. Tibial intramedullary fixation is recommended to maintain the stability of pseudarthrosis [6]. However, current surgical approaches for CPT are not met clinically due to the challenges in realizing and keeping bone healing [7]. Therefore, it is urgent to explore new strategies for CPT therapy.

Inhibition of osteogenic differentiation in CPT-derived mesenchymal stem cells (MSCs) could result in CPT progression [8]. MSCs therapy provides an approach to boost conventional surgical treatments [9,10]. In addition, MSCs derived from patients with CPT often exert a lower ability of osteogenic differentiation compared to MSCs from healthy people [11]. However, the related mechanism remains unclear. Thus, it is essential to investigate how CPT-derived MSCs display a lower ability of osteogenic differentiation.

MicroRNAs (miRNAs), as endogenic noncoding small RNAs, are widely expressed and involved in regulating gene expression [12].

Abbreviation: ADSCs, adipose-derived mesenchymal stem cells; ALP, alkaline phosphatase; CPT, congenital pseudarthrosis of the tibia; ChIP, chromatin immunoprecipitation; HOXD8, Homeobox D8; miRNAs, MicroRNAs; RT-qPCR, Quantitative reverse transcription PCR; MSCs, mesenchymal stem cells; OCN, osteocalcin; OPN, osteopontin; RUNX2, runt-related transcription factor 2; ARS, Alizarin Red S; α-MEM, α-minimum essential medium; DMEM, Dulbecco's modified Eagle's medium; FBS, fetal bovine serum; 3′-UTR, 3′-untranslated region; wt, wild-type; mut, mutant; SD, standard deviation.

* Corresponding author. Department of orthopaedics, Hunan Children's Hospital, No. 86, Ziyuan Road, Yuhua District, Changsha 410007, Hunan Province, PR China
E-mail address: meihaibomb0527@163.com (H. Mei).

Peer review under responsibility of the Japanese Society for Regenerative Medicine.

https://doi.org/10.1016/j.reth.2022.09.005

Accumulating evidence indicated that miRNAs play essential roles in osteogenic differentiation [13,14]. miR-30a is one of the miRNAs that has multiple functions in the cellular process. Liu et al. reported that the miR-30a inhibitor could induce osteogenic differentiation of bone marrow-derived MSCs by targeting Notch1 [15]. Guo et al. demonstrated that miR-30a participates in CircRNA-23525-mediated osteogenic differentiation of adipose-derived MSCs [16]. miR-30a is involved in osteogenic differentiation [15,17]. However, the function of miR-30a in CPT and its underlying mechanism remains mysterious.

mRNAs are involved in CPT progression by modulating the osteogenic differentiation of MSCs [2]. HOXD8 is the pivotal gene in cancer-related pathways and could regulate the osteogenic differentiation of MSCs [18]. Nevertheless, the function of HOXD8 in CPT is largely unknown.

This study illustrated the role of miR-30a in the osteogenic differentiation of MSCs during the progression of CPT. This research might supply a new strategy against CPT.

2. Materials and methods

2.1. MSC isolation, culture, and identification

Patients with CPT and developmental dysplasia of the hip (DDH) were hospitalized at the Division of Orthopedics of Hunan Children's Hospital from June to December 2020. The groups were as follows: CPT group (3 CPT patients with periosteum lesion) and control group (normal iliac periosteum of DDH in 3 cases). This work was approved by the Medical Ethics Committee of Hunan Children's Hospital. Patients and their parents obtained and signed the informed consent. Periosteal tissues were harvested from 3 patients from the CPT or normal group during surgical procedures of osteosynthesis. MSCs were isolated by enzymatic digestion. The unwanted tissues were cut off, and residual blood clots were removed. Then tissue fragments were washed with Hanks' balanced salt solution containing calcium and magnesium. Furthermore, the tissue fragments were cut to ~1 mm. And then the tissues were digested by 2 mg/mL collagenase type II (Gibco, USA) in α-minimum essential medium (α-MEM; Gibco) at 37 °C for 24 h. Digested tissues were centrifuged at 2000 rpm for 5 min, and cells were resuspended by α-MEM containing 10% fetal bovine serum (FBS). Then, cells were plated on a 100 mm dish and cultured. The medium was refreshed every 2–3 days.

MSCs were identified by CD44, CD90, CD31, and CD34 detection, as described previously [19]. Briefly, third-generation periosteal MSCs were digested and resuspended with PBS. Subsequently, the cells were centrifuged at 1500 rpm for 5 min and resuspended with PBS. Cells (100 μL; 1 × 106/mL) were incubated with CD90 (328109), CD44 (397517), CD34 (343519), and CD31 (303115) antibodies (BioLegend, USA). After incubation for 20 min, cells were added with l.5 mL PBS and centrifuged at 2000 rpm for 5 min. After discarded the supernatant, the cells were added with 500 μL PBS for flow cytometry assay (CytoFLEX cytometer, Beckman, USA).

293T cells were derived by the American Type Culture Collection (ATCC, Manassas, VA, USA) and cultured in Dulbecco's modified Eagle's medium (DMEM) (Thermo Fisher, Shanghai, China) including 10% FBS.

2.2. Cell transfection and infection

si-NC, si-HOXD8, miR-NC, miR-30a mimic, and miR-30a inhibitor were obtained from GenePharma (Shanghai, China). MSCs were transfected with si-NC, si-HOXD8, miR-NC, miR-30a mimic, or miR-30a inhibitor by Lipofectamine 2000 (Invitrogen) for 48 h. For HOXD8 overexpression, HOXD8 overexpression lentiviruses (lenti-PLVX-HA-HOXD8) or the corresponding control (lenti-PLVX-HA) were provided by Hanbio Biotechnology Co., Ltd. (Shanghai, China). MSCs (5×10^6/well) were infected with the control (lenti-PLVX-HA) or HOXD8 overexpressed lentiviruses.

2.3. CCK-8 assay

Cells were seeded in 96-well plates at a density of 1000 cells per well. CCK-8 reagents (10 μL; C0037; Beyotime Biotechnology, Shanghai, China) were added and further incubated for 2 h. The absorbance (450 nm) was tested by a microplate reader (Thermo Fisher, USA).

2.4. Osteogenic differentiation of MSCs

Osteogenesis induction was performed using an osteogenic medium (HUXMX-90021, Cyagen Biosciences, China). After 7 days, early osteogenesis was tested via an alkaline phosphatase (ALP) assay kit. After 21 days later, late osteogenic differentiation was detected using the Alizarin Red S (ARS) staining kit (C0148S; Beyotime Technology).

2.5. ALP activity detection

ALP activity was assessed by colorimetric assay and histochemical staining. The ALP kit assay was used to determine ALP activity (MAK447-1 KT; Millipore, Billerica, MA, USA). Cells were washed with PBS and lysed with a lysis buffer. Cell lysates were treated with p-nitrophenyl phosphate at 37 °C. Absorbance was tested by a microplate reader at 405 nm (Thermo Fisher).

For ALP staining, the cells were immobilized in 4% paraformaldehyde at 25 °C for 30 min. The ALP staining kit (M039; Shanghai Gefan Biotechnology Co., Ltd., Shanghai, China) was used to perform ALP staining according to the manufacturer's instructions. Stained cells were examined under a microscope (BX51; Olympus, Tokyo, Japan).

2.6. ARS staining

To detect the matrix mineralization of MSCs, MSCs were fixed in 4% paraformaldehyde at 25 °C for 30 min. Subsequently, the cells were rinsed with PBS thrice and dyed with ARS (C0148S) at 37 °C for 0.5 h [20]. Finally, cells were observed using a microscope (BX51).

2.7. Quantitative reverse transcription-polymerase chain reaction (RT-qPCR)

Total RNA was extracted by TRIzol reagent (TaKaRa, Tokyo, Japan). The PrimeScript RT Reagent Kit (TaKaRa) was used to synthesize first-strand cDNA. Finally, qPCR was measured by the ABI7500 PCR System (Thermo Fisher) with SYBR Green (TaKaRa). In this study, the primers were provided by GenePharma (China). qPCR was performed using the following primers: *HOXD8*: GACCGTTGTTAGCACGCCTT (forward) and CACGTATCGGTCCGTGTTGG (reverse), *miR-30a*: TTCCATACTGCAACGCCATACC (forward) and GCAATCCGC CCTTAGTCCAA (reverse), *RUNX2*: GAACTTTCTGCTGTCTTGGGTG (forward) and GGCAGTAGCTGCGCTGATAG (reverse), *β-actin*: CCTG CGAAACACCTTGATCG (forward) and TCGTCATGTTCCCCACTTCG (reverse), and *U6*: CGTCTTCCCAGGACCGTA (forward) and CGAATC CTGACATTAAGTCG (reverse). β-actin and U6 were adopted as a reference to quantify the mRNA and miR-30a levels, respectively. The $2^{-\Delta\Delta CT}$ method was applied for data quantification.

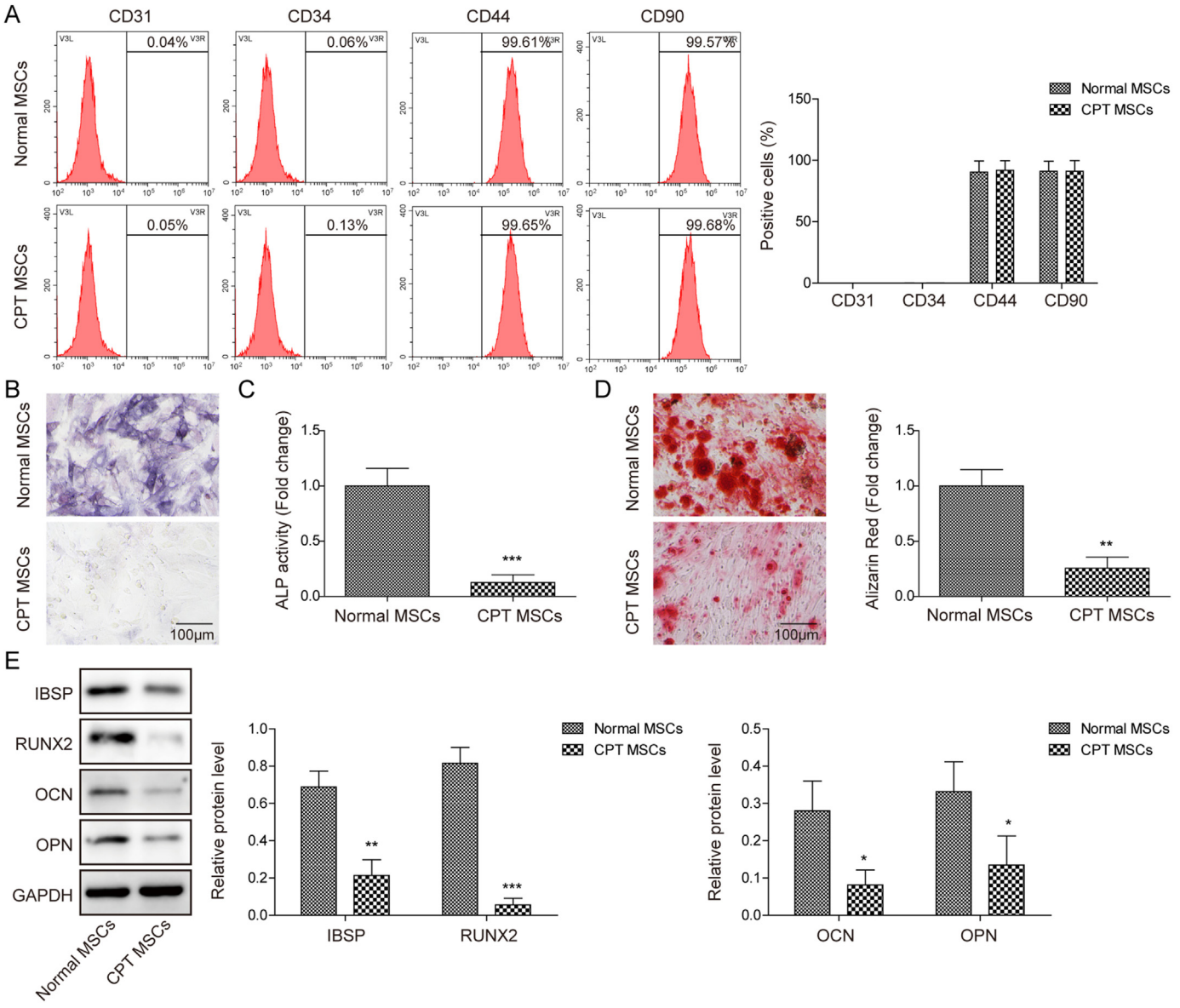

Fig. 1. CPT-derived MSCs exerted a low ability of osteogenic differentiation. (**A**) MSCs were derived from normal or CPT patients. Isolated MSCs were analyzed by flow cytometry. (**B, C**) ALP activity and staining in CPT-derived MSCs were assessed. (**D**) The osteogenic differentiation in CPT-derived MSCs was investigated by Alizarin red staining. (**E**) The levels of IBSP, RUNX2, OCN, and OPN in CPT-derived MSCs were evaluated by Western blot. *$p < 0.05$; **$p < 0.01$; ***$p < 0.001$.

2.8. Western blot

Total protein was homogenized in RIPA buffer (Cell Signaling Technology, Danvers, MA, USA). Next, protein was separated on an SDS-PAGE and transferred to polyvinylidene difluoride membranes. The membranes were incubated with 5% bovine serum albumin in Tris-buffered saline with Tween 20. The membranes were probed with primary antibodies, such as HOXD8 (ab228450; 1:1000; Abcam), RUNX2 (ab236639; 1:1000; Abcam), osteopontin (OPN; ab214050; 1:1000; Abcam), osteocalcin (OCN; ab93876; 1:1000; Abcam), and GAPDH (ab9485; 1:1000; Abcam), and IBSP (#5468; 1:1000; Cell Signaling Technology) at 4 °C overnight. After washing thrice, the membranes were incubated in corresponding horseradish peroxidase-conjugated goat anti-rabbit IgG polyclonal antibody (ab136636; 1:5000; Beyotime Biotechnology) at 25 °C for 1 h. Next, the blots were dyed by the ECL blot kit (Amersham, Cytiva, China) and visualized by the GEL imaging system (Bio-Rad, USA). Finally, protein bands were measured by ImageJ.

2.9. Dual-luciferase reporter assay

The wild-type (wt) and mutant (mut) constructs of the HOXD8 3′-untranslated region (3′-UTR) were linked with psiCHECK-2 vector (Promega, Madison, WI, USA). wt or mut HOXD8 3′-UTR and miR-NC or miR-30a mimics were transfected into 293T cells by Lipofectamine 3000. The luciferase activities were detected by a dual-luciferase reporter assay (Promega).

The wt and mut constructs of the RUNX2 promoter were cloned into psiCHECK-2 vector (Promega). 293T cells were cot-ransfected with the wt or mut RUNX2 promoter vector and HOXD8 overexpression vector by Lipofectamine 3000. The relative luciferase activities were tested by a dual-luciferase reporter assay.

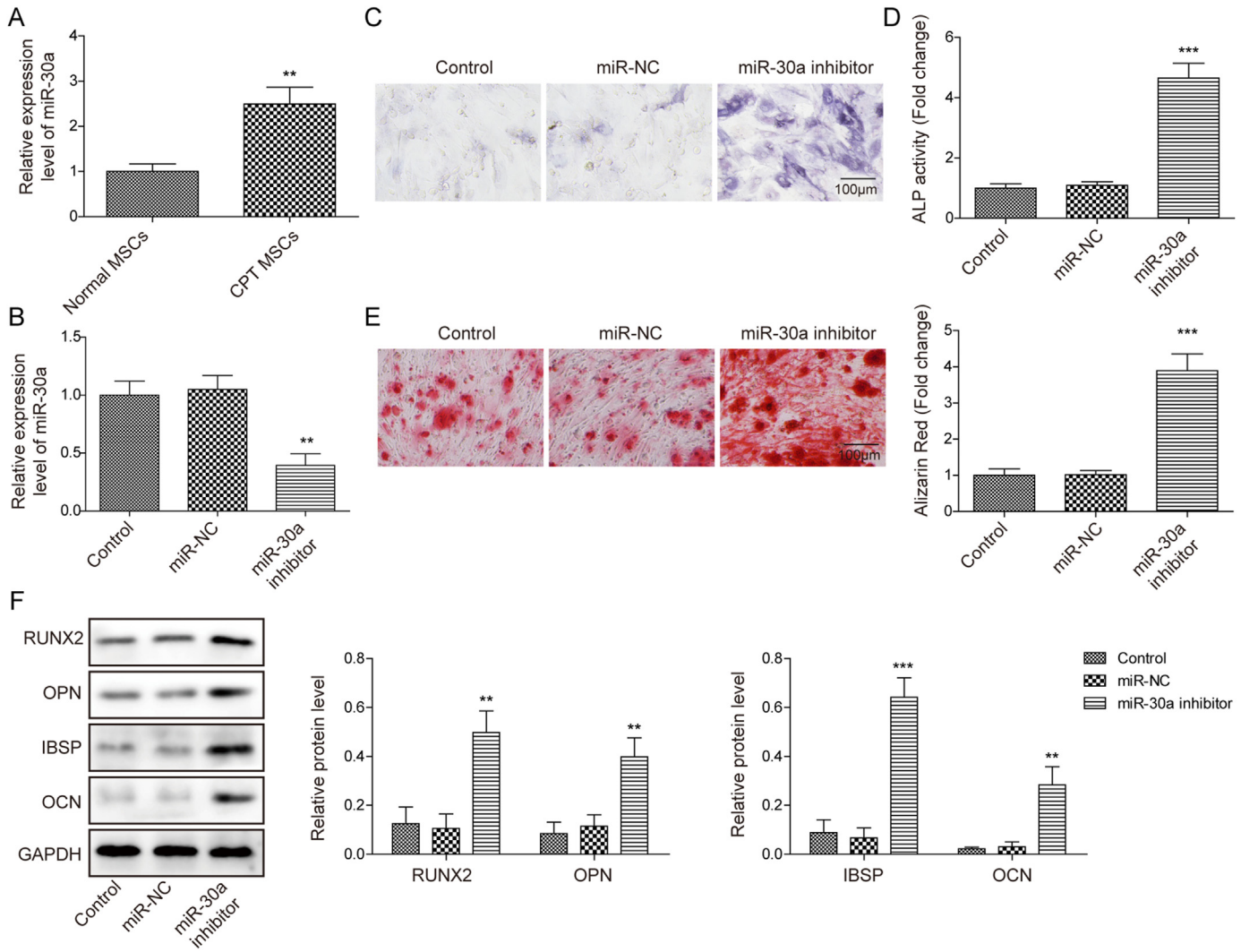

Fig. 2. Downregulation of miR-30a promoted the osteogenic differentiation of MSCs. (**A**) The expression level of miR-30a in CPT-derived MSCs was tested via RT-qPCR. MSCs were transfected with NC or miR-30a inhibitor. (**B**) The expression of miR-30a in MSCs was assessed via RT-qPCR. (**C, D**) ALP activity and staining in CPT-derived MSCs were assessed. (**E**) The osteogenic differentiation in MSCs was investigated by ARS staining. (**F**) The levels of IBSP, RUNX2, OCN, and OPN in MSCs were evaluated by Western blot. *$p < 0.05$; **$p < 0.01$; ***$p < 0.001$.

2.10. Chromatin immunoprecipitation (ChIP)

ChIP was performed according to the instructions provided by the ChIP Assay Kit (Millipore). Briefly, the cells were treated with a lysis buffer on ice for 10 min. Subsequently, the cell lysates were sonicated for seven 5 s pulses on ice using Sonicator 3000 (Misonix, Farmingdale, NY, USA) and acquired 200 to 1000 bp DNA fragments. The cell lysates were precleared with ChIP buffer, agarose beads and protease inhibitor cocktail on ice for 1 h. The cleared lysates were then incubated with antibodies against HOXD8 (ab228450; Abcam) or normal mouse IgG (ab37355; Abcam) at 4 °C for 12 h. Next, 60 μL of Protein A agarose/salmon sperm DNA slurry was added with rotation for 1 h at 4 °C. The beads were washed sequentially with low-salt wash buffer (150 mM), high-salt wash buffer (500 mM), LiCl wash buffer, and TE buffer. Subsequently, the mixture was washed with eluate buffer. The cross-linking was reversed using 5 M NaCl and incubated at 65 °C for 4 h. Finally, the samples were treated with RNase A and used for qPCR to detect the level of the RUNX2 promoter.

2.11. Statistical analysis

GraphPad Prism 7 was applied to analyze the data. All values were conducted at least three times and the data were expressed as means ± standard deviation (SD). Comparisons between two groups were analyzed using the unpaired Student's t-test. Comparisons of more than two groups were analyzed by one-way analysis of variance, followed by Tukey's post hoc test. $p < 0.05$ was considered statistically significant.

3. Results

3.1. CPT-derived MSCs exerted a low ability of osteogenic differentiation

MSCs were derived from the periosteum of CPT patients, and flow cytometry was applied to identify MSCs. As revealed in Fig. 1A, flow cytometry results showed that CD44 (>99.61%) and CD90 (>99.57%) were significantly expressed in the isolated cells,

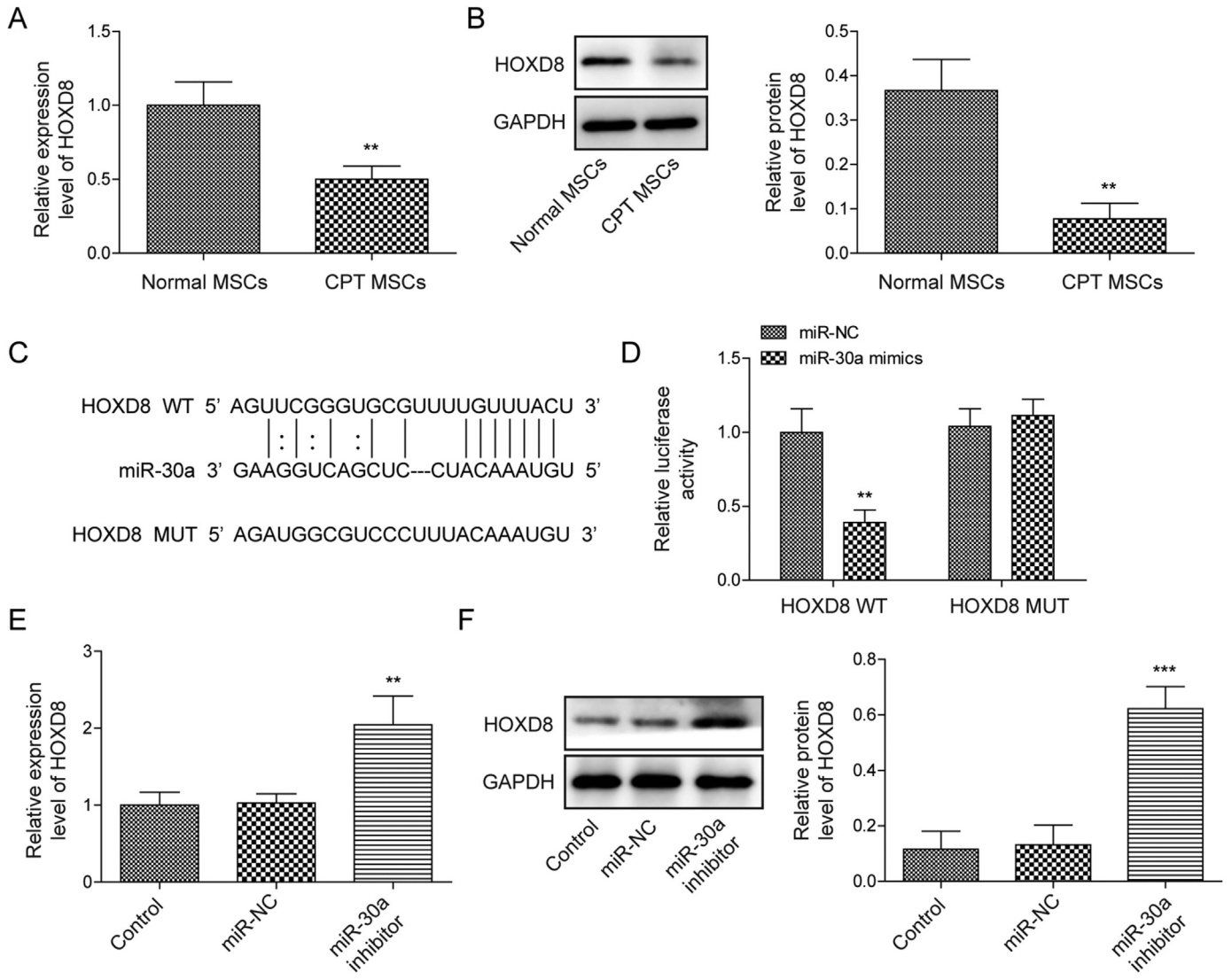

Fig. 3. HOXD8 was targeted by miR-30a. (**A, B**) HOXD8 level in CPT-derived MSCs was evaluated by RT-qPCR and Western blot. (**C**) The binding sites between miR-30a and HOXD8 via TargetScan. (**D**) Dual-luciferase reporter assay was conducted to investigate the relation between miR-30a and HOXD8. CPT-derived MSCs were treated with the miR-30a inhibitor. (**E, F**) HOXD8 expression level in MSCs was evaluated via RT-qPCR and Western blot. *$p < 0.05$; **$p < 0.01$; ***$p < 0.001$.

whereas CD31 (<0.06%) and CD34 (<0.13%) were rarely detected, indicating that MSCs were successfully isolated. The ALP activity in CPT-derived MSCs was significantly lower than in normal iliac periosteum-derived MSCs (Fig. 1B and C). Consistently, CPT-derived MSCs showed a lower ability of osteogenic differentiation than normal iliac periosteum-derived MSCs (Fig. 1D). The cell viability of CPT-derived MSCs was slightly lower than normal iliac periosteum-derived MSCs, but there was no obvious difference (Supplementary Fig. S1). Furthermore, the protein expressions of osteogenic markers (OCN, IBSP, RUNX2, and OPN) [21,22] in CPT-derived MSCs on day 14 were significantly downregulated compared to those in normal iliac periosteum-derived MSCs (Fig. 1E). In sum, the ability of osteogenic differentiation in CPT-derived MSCs was much lower than in normal iliac periosteum-derived MSCs.

3.2. miR-30a knockdown notably induced the osteogenic differentiation of MSCs

Accumulating evidence suggested that miR-30a plays crucial functions in the osteogenic differentiation of MSCs [23]. miR-30a expression was detected in CPT-derived MSCs or normal iliac periosteum-derived MSCs. In Fig. 2A, miR-30a was upregulated in CPT-derived MSCs. To evaluate the function of miR-30a in CPT, CPT-derived MSCs were transfected with the miR-30a inhibitor. miR-30a in MSCs was markedly decreased by the miR-30a inhibitor (Fig. 2B), and the miR-30a inhibitor remarkably upregulated the ALP activity of CPT-derived MSCs (Fig. 2C and D). Consistently, downregulation of miR-30a significantly promoted the osteogenic differentiation of CPT-derived MSCs (Fig. 2E). Furthermore, the levels of OCN, IBSP, RUNX2 and OPN in CPT-derived MSCs were remarkably increased in the presence of miR-30a inhibitor (Fig. 2F). In sum, downregulation of miR-30a remarkably promoted the osteogenic differentiation of CPT-derived MSCs.

3.3. miR-30a targeted to HOXD8

Next, we aimed to explore the underlying mechanism of miR-30a in regulating the osteogenic differentiation of CPT-derived MSCs. HOXD8 was involved in modulating the osteogenic differentiation of MSCs [18]. In Fig. 3A and B, the expression level of

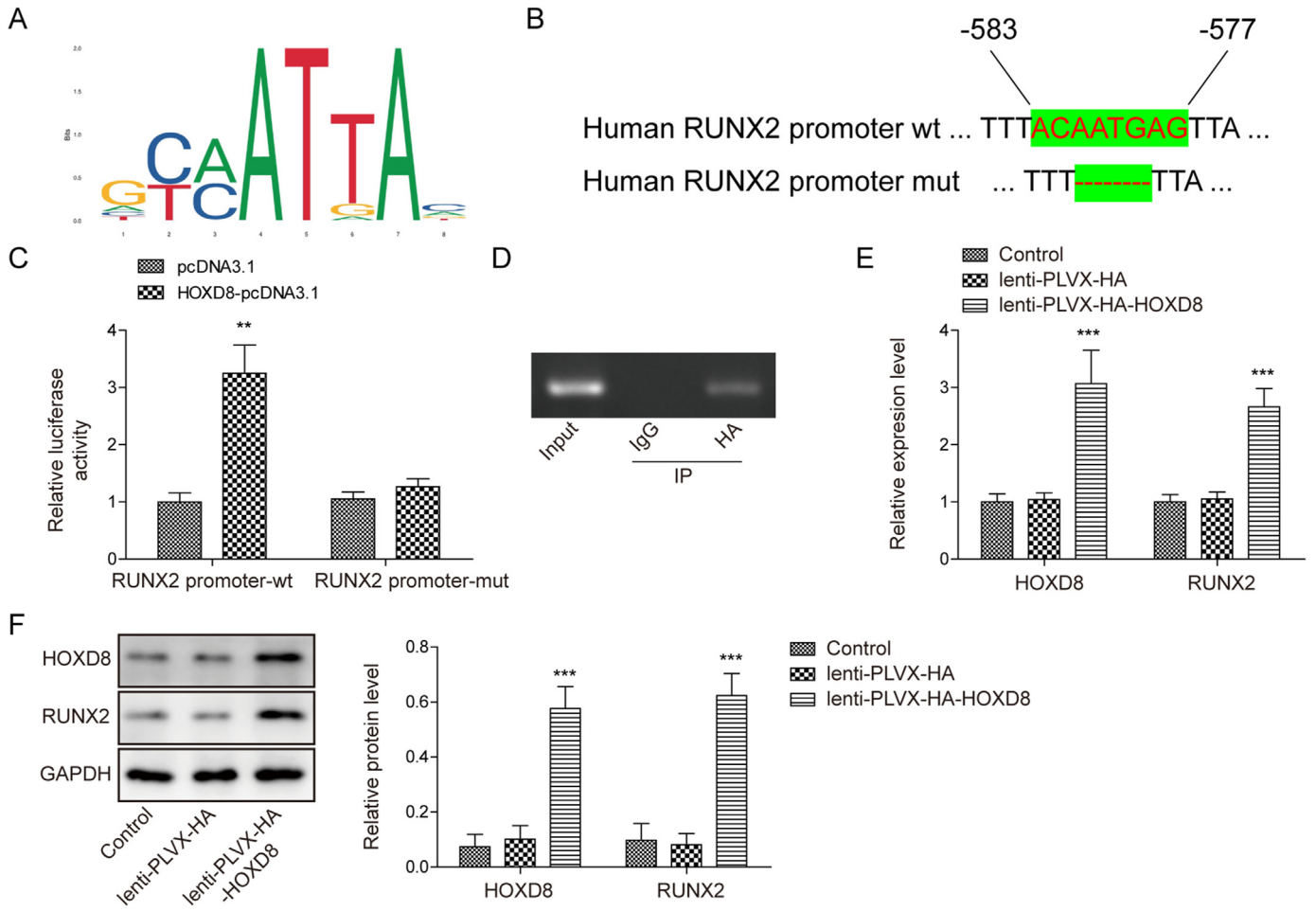

Fig. 4. HOXD8 transcriptionally activated RUNX2. (**A**) JASPAR was applied to analyze the binding motif of HOXD8. (**B**) The potential binding sequences between HOXD8 and RUNX2 promoter were performed by JASPAR. (**C**) Luciferase activity in RUNX2 promoter was investigated via dual-luciferase reporter assay. (**D**) The relation between HOXD8 and RUNX2 promoter was detected via ChIP. MSCs were overexpressed with HOXD8 by lentivirus. (**E, F**) The expressions of HOXD8 and RUNX2 in CPT-derived MSCs were assessed via RT-qPCR and Western blot. $*p < 0.05$; $**p < 0.01$; $***p < 0.001$.

HOXD8 in CPT-derived MSCs was notably lower than in normal MSCs. A sequence of the targeted sites in the miR-30a and HOXD8 3′-UTR regions was predicted by the TargetScan database (Fig. 3C). Luciferase assay confirmed that overexpression of miR-30a significantly inhibited luciferase activity in the wt HOXD8 3′-UTR group but had no effect on luciferase activity in the mut HOXD8 3′-UTR group (Fig. 3D). Furthermore, the downregulation of miR-30a upregulated the expression of HOXD8 in MSCs (Fig. 3E and F). Taken together, HOXD8 was identified to be the downstream mRNA of miR-30a.

3.4. HOXD8 transcriptionally activated RUNX2

A previous study indicated that HOXD8 could promote osteogenic differentiation via the activation of RUNX2 in adolescent idiopathic scoliosis [18]. Thus, the relation between HOXD8 and RUNX2 in CPT was further investigated. In Fig. 4A and B, HOXD8 had a potential binding sequence to the region of the RUNX2 promoter by using JASPAR prediction. Meanwhile, the luciferase activity in wt-RUNX2 was significantly promoted by pcDNA3.1-HOXD8 (Fig. 4C). HOXD8 was found to bind to the promoter of RUNX2 (Fig. 4D), and overexpression of HOXD8 notably upregulated the levels of RUNX2 and HOXD8 in MSCs (Fig. 4E and F). In sum, HOXD8 could upregulate RUNX2 by transcriptionally activating RUNX2.

3.5. miR-30a restrained osteogenic differentiation by negatively modulating HOXD8

To further confirm the mechanism of miR-30a in modulating the osteogenic differentiation of CPT-derived MSCs, CPT-derived MSCs were transfected with the miR-30a inhibitor or HOXD8 siRNA. In Fig. 5A and B, the level of miR-30a in CPT-derived MSCs was significantly reduced by the miR-30a inhibitor. In contrast, miR-30a downregulation upregulated the expression of HOXD8, which was abolished by HOXD8 knockdown. In addition, miR-30a inhibitor-induced upregulation of ALP activity and osteogenic differentiation were reversed by HOXD8 knockdown (Fig. 5C–E). Furthermore, miR-30a downregulation-induced upregulation of OPN, OCN, RUNX2, and IBSP in MSCs was rescued by HOXD8 knockdown (Fig. 5F). To sum up, miR-30a inhibited the osteogenic differentiation of CPT-derived MSCs by negatively regulating HOXD8 (Fig. 6).

4. Discussion

CPT-derived MSCs play important roles in progression of CPT [8,24]. In this study, miR-30a downregulation promoted the osteogenic differentiation of CPT-derived MSCs, and miR-30a could directly target HOXD8. In addition, HOXD8 could transcriptionally activate RUNX2. Thus, this study investigated the role of miR-30a in CPT and found that miR-30a could act as a crucial mediator in CPT.

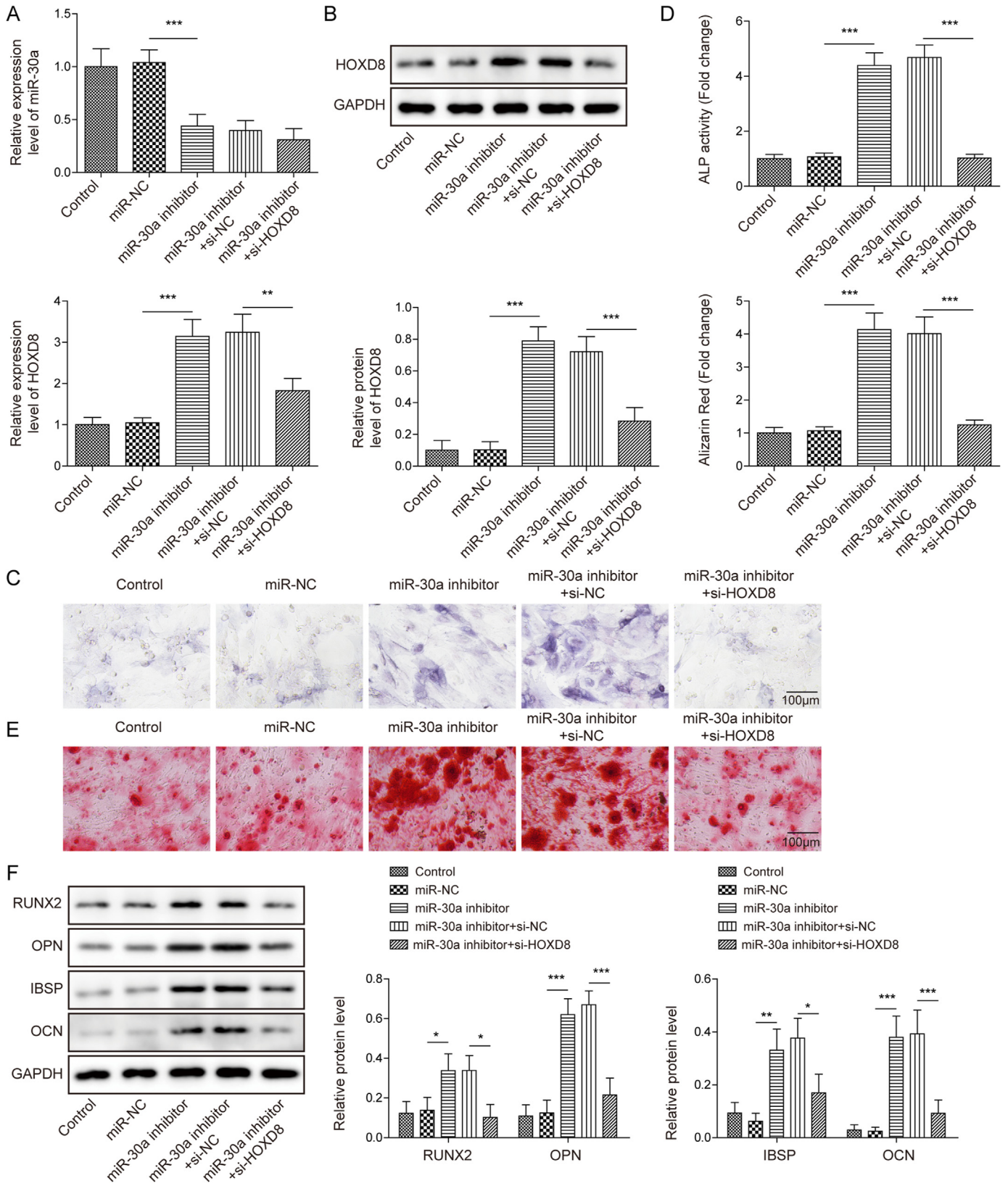

Fig. 5. miR-30a downregulated the osteogenic differentiation of CPT-derived MSCs by inactivating HOXD8. MSCs were treated with miR-NC, miR-30a inhibitor, miR-30a inhibitor + si-NC or miR-30a inhibitor + si-HOXD8. (**A, B**) miR-30a or HOXD8 level in MSCs was detected by RT-qPCR or Western blot. (**C, D**) ALP activity and staining in CPT-derived MSCs were assessed. (**E**) The osteogenic differentiation in MSCs was investigated by ARS staining. (**F**) The levels of IBSP, RUNX2, OCN and OPN in MSCs were detected by Western blot. *$p < 0.05$; **$p < 0.01$; ***$p < 0.001$.

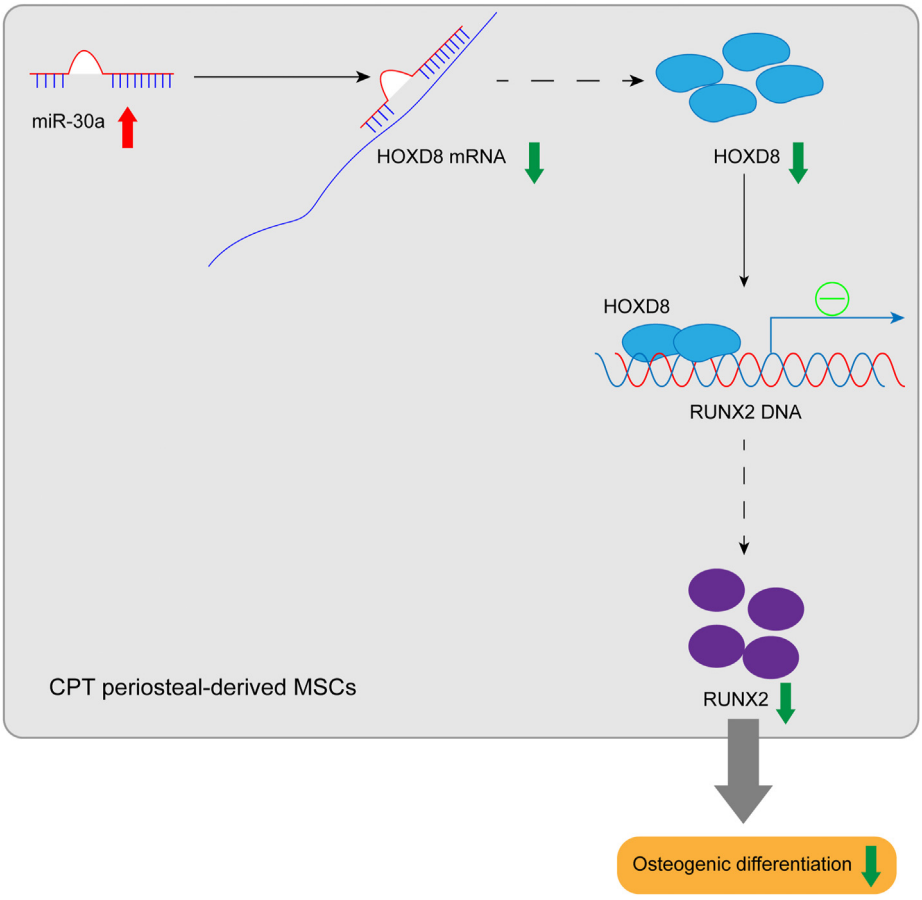

Fig. 6. Mechanism of miR-30a regulating osteogenic differentiation. miR-30a negatively regulates HOXD8 by targeting HOXD8, and HOXD8 could transcriptionally activate RUNX2. The downregulated RUNX2 inhibited the osteogenic differentiation of CPT-derived MSCs.

miRNAs are involved in osteogenic differentiation [25,26]. miR-22 could induce the osteogenic differentiation of valvular interstitial cells by downregulation of CAB39 during aortic valve calcification [27]. miR-339-5p could inhibit osteogenic differentiation during the development of osteoporosis [28]. Zhang et al. have reported that miR-30a suppressed BMP9-induced osteogenic differentiation [23]. It was suggested that miR-30a-5p modulated the osteogenic differentiation potential in HUVECs by downregulation of SLUG, VIMENTIN and RUNX2 [17]. This study revealed that the miR-30a inhibitor could promote the osteogenic differentiation of CPT-derived MSCs. Thus, results further supplemented the function of miR-30a in CPT.

HOXD8 is a crucial mediator in cellular processes, especially tumor progression [29,30]. Additionally, HOXD8 has been reported to act as a promoter in the osteogenic differentiation of MSCs [18]. This study indicated that HOXD8 was the downstream mRNA of miR-30a in CPT, and miR-30a could regulate the osteogenic differentiation of CPT-derived MSCs by negatively regulating HOXD8.

Runx2 plays a vital role in osteogenic differentiation [31,32]. For instance, blocking the NLRP3 inflammasome could reduce osteogenic differentiation via inhibition of RUNX2 [33]. IRF4 could suppress osteogenic differentiation of BM-MSCs by inactivating RUNX2 [34]. CircRNA-23525 modulated RUNX2 expression by targeting miR-30a-3p, leading to positive regulation in the osteoblastic differentiation of adipose-derived mesenchymal stem cells (ADSCs) [16]. This study proved that HOXD8 could bind to RUNX2, and RUNX2 was transcriptionally activated by HOXD8. Data confirmed that upregulation of HOXD8 could induce the osteogenic differentiation of CPT-derived MSCs via RUNX2 activation.

In summary, this study demonstrated that miR-30a inhibits the osteogenic differentiation of CPT-derived MSCs by targeting HOXD8, which might provide new ideas for discovering new methods for CPT treatment.

Ethics statement

This work was approved by the Medical Ethics Committee of Hunan Children's Hospital.

Funding

This work was supported by Major science and technology project for collaborative prevention and control of birth defects in Hunan Province (2019SK1010). Key Research and Development Program of Hunan Province(2020SK2113) Clinical Research Center for Limb Deformity of Children in Hunan Province(2019SK4006). National Key Clinical Specialty Construction Project - Pediatric Surgery of Hunan Children's Hospital (XWYF [2022] No. 2).

Declaration of competing interest

The authors declare that they have no known competing financial interests or personal relationships that could have appeared to influence the work reported in this paper.

Acknowledgements

We would like to give our sincere gratitude to the reviewers for their constructive comments.

Appendix A. Supplementary data

Supplementary data to this article can be found online at https://doi.org/10.1016/j.reth.2022.09.005.

References

[1] Hu X, Li A, Liu K, Mei H. Efficacy comparison of 3 kinds of distal tibial hemiepiphyseal implants in the treatment of postoperative ankle valgus of congenital pseudarthrosis of the tibia. J Pediatr Orthop 2022;42(5):e441–7.
[2] Zheng Y, Zhu G, Liu Y, Zhao W, Yang Y, Luo Z, et al. Case series of congenital pseudarthrosis of the tibia unfulfilling neurofibromatosis type 1 diagnosis: 21% with somatic nf1 haploinsufficiency in the periosteum. Hum Genet 2022;141(8):1371–83.
[3] Hefti F, Bollini G, Dungl P, Fixsen J, Grill F, Ippolito E, et al. Congenital pseudarthrosis of the tibia: History, etiology, classification, and epidemiologic data. J Pediatr Orthop B 2000;9(1):11–5.
[4] Lippross S, Tsaknakis K, Lorenz HM, Hell AK. Congenital pseudarthrosis of the tibia : A rare often underestimated disorder. Unfallchirurg 2021;124(9):755–67.
[5] Paley D. Congenital pseudarthrosis of the tibia: Biological and biomechanical considerations to achieve union and prevent refracture. J Child Orthop 2019;13(2):120–33.
[6] Liu Y, Yang G, Zhu G, Tan Q, Wu J, Liu K, et al. Application of the "telescopic rod" in a combined surgical technique for the treatment of congenital pseudarthrosis of the tibia in children. J Orthop Surg Res 2021;16(1):532.
[7] Das SP, Ganesh S, Pradhan S, Singh D, Mohanty RN. Effectiveness of recombinant human bone morphogenetic protein-7 in the management of congenital pseudoarthrosis of the tibia: A randomised controlled trial. Int Orthop 2014;38(9):1987–92.
[8] Granchi D, Devescovi V, Baglio SR, Leonardi E, Donzelli O, Magnani M, et al. Biological basis for the use of autologous bone marrow stromal cells in the treatment of congenital pseudarthrosis of the tibia. Bone 2010;46(3):780–8.
[9] Velarde F, Ezquerra S, Delbruyere X, Caicedo A, Hidalgo Y, Khoury M. Mesenchymal stem cell-mediated transfer of mitochondria: Mechanisms and functional impact. Cell Mol Life Sci 2022;79(3):177.
[10] Zhu T, Hu Z, Wang Z, Ding H, Li R, Wang J, et al. Microrna-301b-3p from mesenchymal stem cells-derived extracellular vesicles inhibits txnip to promote multidrug resistance of gastric cancer cells. Cell Biol Toxicol 2022.
[11] Memeo A, Verdoni F, Minoli CF, Voto A, D'Amato RD, Formiconi F, et al. Effectiveness of bone marrow aspirate concentrate (bmac) as adjuvant therapy in the surgical treatment of congenital pseudoarthrosis of the tibia: A retrospective comparative study. J Biol Regul Homeost Agents 2020;34(4 Suppl 3):431–40.
[12] Yang D, Deschenes I, Fu JD. Multilayer control of cardiac electrophysiology by microrna. J Mol Cell Cardiol 2022;166:107–15.
[13] Chen Z, Lin W, Zhao S, Mo X, Wen Z, Cheung WH, et al. Identification of circrna expression profiles in bmscs from glucocorticoid-induced osteoporosis model. Stem Cells Int 2022;2022:3249737.
[14] Dai Z, Wei G. Inhibition of mirna-100 facilitates bone regeneration defects of mesenchymal stem cells in osteoporotic mice through the protein kinase b pathway. Bioengineered 2022;13(1):963–73.
[15] Che M, Gong W, Zhao Y, Liu M. Long noncoding rna hcg18 inhibits the differentiation of human bone marrow-derived mesenchymal stem cells in osteoporosis by targeting mir-30a-5p/notch1 axis. Mol Med 2020;26(1):106.
[16] Guo Z, Zhao L, Ji S, Long T, Huang Y, Ju R, et al. Circrna-23525 regulates osteogenic differentiation of adipose-derived mesenchymal stem cells via mir-30a-3p. Cell Tissue Res 2021;383(2):795–807.
[17] Ciavarella C, Motta I, Vasuri F, Fittipaldi S, Valente S, Pollutri D, et al. Involvement of mir-30a-5p and mir-30d in endothelial to mesenchymal transition and early osteogenic commitment under inflammatory stress in huvec. Biomolecules 2021;11(2):226.
[18] Zhuang Q, Ye B, Hui S, Du Y, Zhao RC, Li J, et al. Long noncoding rna lncais downregulation in mesenchymal stem cells is implicated in the pathogenesis of adolescent idiopathic scoliosis. Cell Death Differ 2019;26(9):1700–15.
[19] Yu Y, Li M, Zhou Y, Shi Y, Zhang W, Son G, et al. Activation of mesenchymal stem cells promotes new bone formation within dentigerous cyst. Stem Cell Res Ther 2020;11(1):476.
[20] Zhao G, Luo WD, Yuan Y, Lin F, Guo LM, Ma JJ, et al. Linc02381, a sponge of mir-21, weakens osteogenic differentiation of huc-mscs through klf12-mediated wnt4 transcriptional repression. J Bone Miner Metab 2022;40(1):66–80.
[21] Toor RH, Malik S, Qamar H, Batool F, Tariq M, Nasir Z, et al. Osteogenic potential of hexane and dichloromethane fraction of cissus quadrangularis on murine preosteoblast cell line mc3t3-e1 (subclone 4). J Cell Physiol 2019;234(12):23082–96.
[22] Toor RH, Tasadduq R, Adhikari A, Chaudhary MI, Lian JB, Stein JL, et al. Ethyl acetate and n-butanol fraction of cissus quadrangularis promotes the mineralization potential of murine pre-osteoblast cell line mc3t3-e1 (subclone 4). J Cell Physiol 2019;234(7):10300–14.
[23] Zhang R, Weng Y, Li B, Jiang Y, Yan S, He F, et al. Bmp9-induced osteogenic differentiation is partially inhibited by mir-30a in the mesenchymal stem cell line c3h10t1/2. J Mol Histol 2015;46(4-5):399–407.
[24] Granchi D, Devescovi V, Baglio SR, Magnani M, Donzelli O, Baldini N. A regenerative approach for bone repair in congenital pseudarthrosis of the tibia associated or not associated with type 1 neurofibromatosis: Correlation between laboratory findings and clinical outcome. Cytotherapy 2012;14(3):306–14.
[25] Bin-Bin Z, Da-Wa ZX, Chao L, Lan-Tao Z, Tao W, Chuan L, et al. M2 macrophagy-derived exosomal mirna-26a-5p induces osteogenic differentiation of bone mesenchymal stem cells. J Orthop Surg Res 2022;17(1):137.
[26] Dalle Carbonare L, Bertacco J, Minoia A, Cominacini M, Bhandary L, Elia R, et al. Modulation of mir-204 expression during chondrogenesis. Int J Mol Sci 2022;23(4):2130.
[27] Yang F, Liu S, Gu Y, Yan Y, Ding X, Zou L, et al. Microrna-22 promoted osteogenic differentiation of valvular interstitial cells by inhibiting cab39 expression during aortic valve calcification. Cell Mol Life Sci 2022;79(3):146.
[28] Li M, Li C, Zheng H, Zhou Z, Yang W, Gong Y, et al. Circrna_0001795 sponges mirna-339-5p to regulate yes-associated protein 1 expression and attenuate osteoporosis progression. Bioengineered 2022;13(2):2803–15.
[29] Xu Y, Tsai CW, Chang WS, Han Y, Huang M, Pettaway CA, et al. Epigenome-wide association study of prostate cancer in african americans identifies DNA methylation biomarkers for aggressive disease. Biomolecules 2021;11(12):1826.
[30] Zhang Y, Yu Y, Su X, Lu Y. Hoxd8 inhibits the proliferation and migration of triple-negative breast cancer cells and induces apoptosis in them through regulation of akt/mtor pathway. Reprod Biol 2021;21(4):100544.
[31] Kong W, Tang Y, Tang K, Yan Z, Liu T, Tao Q, et al. Leukemia inhibitory factor is dysregulated in ankylosing spondylitis and contributes to bone formation. Int J Rheum Dis 2022;25(5):592–600.
[32] Xu L, Wu J, Yu Y, Li H, Sun S, Zhang T, et al. Dok5 regulates proliferation and differentiation of osteoblast via canonical wnt/beta-catenin signaling. J Musculoskelet Neuronal Interact 2022;22(1):113–22.
[33] Lu J, Xie S, Deng Y, Xie X, Liu Y. Blocking the nlrp3 inflammasome reduces osteogenic calcification and m1 macrophage polarization in a mouse model of calcified aortic valve stenosis. Atherosclerosis 2022;347:28–38.
[34] Zhang X, Zhang Y, Yang L, Wu Y, Ma X, Tong G, et al. Irf4 suppresses osteogenic differentiation of bm-mscs by transcriptionally activating mir-636/dock9 axis. Clinics (Sao Paulo) 2022;77:100019.